Vapor-Liquid Equilibria of Toluene–Ethyl Alcohol and Benzene–Ethyl Alcohol

JOSEPH C. LANDWEHR[1], STEPHEN YERAZUNIS, and HARRY H. STEINHAUSER, Jr.
Department of Chemical Engineering, Rensselaer Polytechnic Institute, Troy, N. Y.

Distillation has been and continues to be a separation method of widespread use in the chemical and petroleum industries. The design of distillation equipment to effect separations or to recover solvents requires a knowledge of vapor-liquid equilibrium compositions. With this in mind, the purpose of the investigation reported here was to obtain the necessary data for the construction of the equilibrium diagrams of two binary systems. Equilibrium data for the ethyl alcohol–toluene system at 756 mm. of mercury and the ethyl alcohol-benzene system at 760 mm. of mercury are reported.

MATERIALS

Benzene and toluene, c.p. grade, were purified by distillation in a Podbielniak Hyper-Cal, high temperature fractionating apparatus with a 72-inch wire-packed distilling tube. The purified benzene had a refractive index of 1.49657 ± 0.00005 at 27°C. and the toluene had an index of 1.49255 ± 0.00005, both in good agreement with published values (*8*). The c.p. ethyl alcohol azeotrope was distilled in the Podbielniak column along with benzene as an azeotroping agent. The product had a refractive index of 1.35843 ± 0.00005, in good agreement with published values (*8*).

ANALYTICAL METHODS

Vapor and liquid samples were analyzed by means of refractive index using a Bausch & Lomb precision refractometer with a monochromatic sodium *D* line light source. Calibration curves were constructed by plotting the difference in composition at constant refractive index between the experimental refractive index *vs.* composition curve and the straight-line value against the straight-line value. The refractive index–composition data are given in Table I.

To make up standard mixtures for constructing the calibration curves, one component was drawn into an evacuated tube from a storage bottle, without direct contact with the atmosphere. The tube was weighed before and after introducing the first component. The second component was introduced in a similar fashion and the tube was weighed again. The samples were placed in a constant temperature bath until thermal equilibrium was reached. The indices of refraction were then determined.

APPARATUS

The equilibrium still, designed by Langdon and Yerazunis in 1948, is shown in Figure 1. The still is a recirculation type utilizing the Cottrell pump principle. It is a modification of the Gillespie still (*4*), in that the liquid sampling point has been separated from the reboiler. This feature has also been included by Fowler (*3*) and Ellis (*2*). Vapor and liquid in equilibrium at the top of the Cottrell pump are cleanly separated in a reverse bend separator. The separator jacket was evacuated and lagged to prevent refluxing.

The pressure was maintained constant within ±0.1 mm. of

Table I. Refractive Index-Composition Data at 27°C. for Systems Ethyl Alcohol-Benzene and Ethyl Alcohol-Toluene

Mole Fraction Ethyl Alcohol	Refractive Index for System	
	Benzene	Toluene
0.0	1.49657	1.49255
0.175	1.47872	...
0.2173	...	1.47434
0.291	1.46601	...
0.3273	...	1.46374
0.461	1.44545	...
0.4869	...	1.44628
0.575	1.43023	...
0.658	1.41826	...
0.6598	...	1.42422
0.7732	...	1.40509
0.843	1.38883	...
0.9084	...	1.37919
0.911	1.37610	...
0.9322	...	1.37412
1.0	1.35843	1.35843

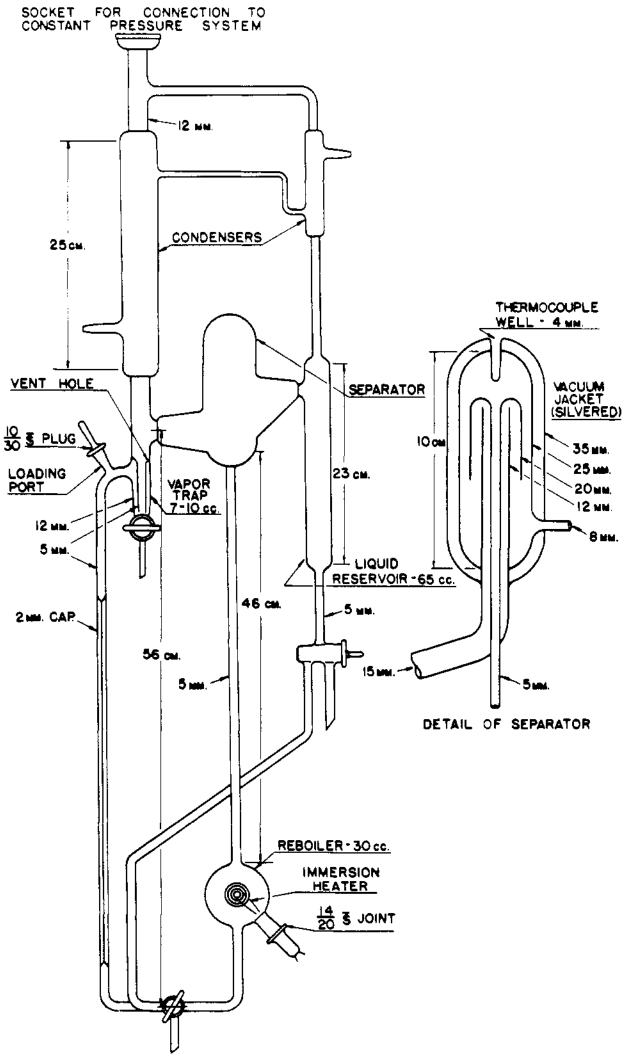

Figure 1. Equilibrium still

---

[1] Present address, Lion Oil Co., El Dorado, Ark.

Table II. Vapor Liquid Equilibrium Data for the System Toluene–Ethyl Alcohol

Temp., °C.	Mole Fraction Ethyl Alcohol		Relative Volatility Toluene to Ethyl Alcohol	Log Activity Coefficient	
	In liquid	In vapor		Toluene	Ethyl alcohol
110.6	0.0	0.0	...	...	...
91.06	0.0666	0.4478	0.0879	0.0195	0.6075
88.20	0.0908	0.5083	0.0967	0.0276	0.5809
87.45	0.0985	0.5224	0.0998	0.0294	0.5687
85.60	0.1191	0.5570	0.1076	0.0334	0.5444
83.40	0.1576	0.5991	0.1252	0.0415	0.4907
80.60	0.2523	0.6536	0.1788	0.0772	0.3711
79.10	0.3469	0.6830	0.2465	0.1139	0.2783
78.40	0.4283	0.7018	0.3185	0.1549	0.2093
77.95	0.4890	0.7141	0.3834	0.1930	0.1676
77.30	0.6330	0.7444	0.5924	0.2980	0.0849
77.04	0.7310	0.7751	0.7886	0.3813	0.0442
77.00	0.8082	0.8094	0.9920	0.4569	0.0208
77.15	0.8794	0.8554	1.232	0.5362	0.0048
77.40	0.9262	0.8975	1.433	0.5962	−0.0003
77.45	0.9382	0.9099	1.503	0.6158	−0.0017
77.60	0.9545	0.9304	1.569	0.6352	−0.0013
78.3	1.0	1.0	...	...	...

Table III. Vapor Liquid Equilibrium Data for the System Benzene–Ethyl Alcohol

Temp., °C.	Mole Fraction Ethyl Alcohol		Relative Volatility Benzene to Ethyl Alcohol	Log Activity Coefficient	
	In liquid	In vapor		Benzene	Ethyl alcohol
80.1	0.0	0.0	...	0.0	...
75.55	0.030	0.142	0.185	0.0080	0.728
72.3	0.065	0.244	0.216	0.0142	0.678
70.4	0.114	0.309	0.288	0.0255	0.572
68.7	0.216	0.374	0.460	0.0604	0.408
68.15	0.317	0.410	0.670	0.1034	0.290
68.0	0.406	0.435	0.887	0.1471	0.212
68.0	0.544	0.480	1.292	0.226	0.1275
68.45	0.639	0.515	1.664	0.290	0.0806
69.4	0.749	0.575	2.21	0.377	0.0412
70.6	0.828	0.642	2.67	0.447	0.0250
72.7	0.896	0.740	3.04	0.501	0.0145
74.8	0.943	0.837	3.24	0.531	0.0087
76.15	0.968	0.900	3.30	0.541	0.0057
77.15	0.984	0.948	3.45	0.560	0.0035
78.3	1.000	1.000	...	...	0.0

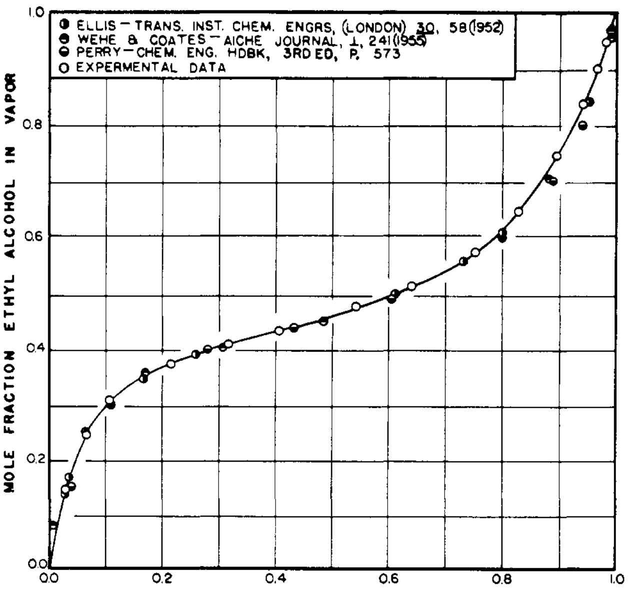

Figure 2. Vapor-liquid equilibrium diagram for the benzene-ethyl alcohol system at 760 mm. of mercury

mercury by an electronic apparatus previously described (*1*). Temperatures were measured to within ±0.2°C. with a copper-constantan thermocouple calibrated against a thermometer certified by the National Bureau of Standards.

PROCEDURE

Each system was run off in two parts; one over a range of liquid composition from pure component A to approximately 0.5 mole fraction, and the other from pure component B over the remainder of the composition range. About 16 points were obtained for each system. The boiling point in the still for each pure component was first obtained. Ninety milliliters of the pure component were charged to the still for the boiling point determination. To effect a shift in composition, after the above determination was made, a few milliliters of the second component were introduced through a port located just after the vapor trap in the vapor return line. One hour was allowed for equilibrium to be established. Temperature measurements were taken every 2 or 3 minutes during the last 15 minutes of the run, and the constancy of these readings indicated that equilibrium existed. Power to the immersion heater was then shut off and a vapor and a liquid sample were collected in stoppered test tubes. The procedure was repeated until seven or eight points were obtained in each range of composition.

RESULTS

Equilibrium vapor-liquid compositions determined in this investigation are reported in Tables II and III along with the activity coefficient data calculated from the experimental results. The experimental data are also presented in Figures 2 and 3 as equilibrium vapor composition *vs.* liquid composition and in Figures 4 and 5 as temperature-composition diagrams. The activity coefficients for the two components were calculated from:

$$\gamma = yP_t/xP$$

where

γ = activity coefficient
y = mole fraction of component in vapor
x = mole fraction of component in liquid
P_t = total pressure
P = vapor pressure of component at equilibrium temperature

The activity coefficient–composition data are presented

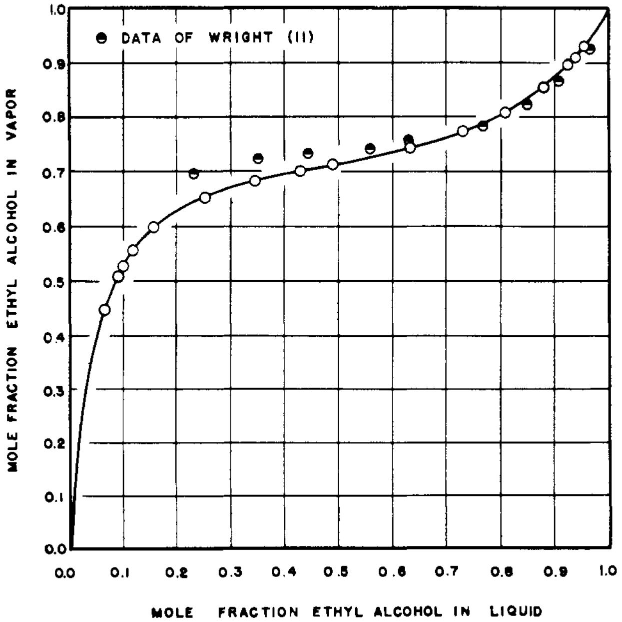

Figure 3. Vapor-liquid equilibrium diagram for toluene–ethyl alcohol system

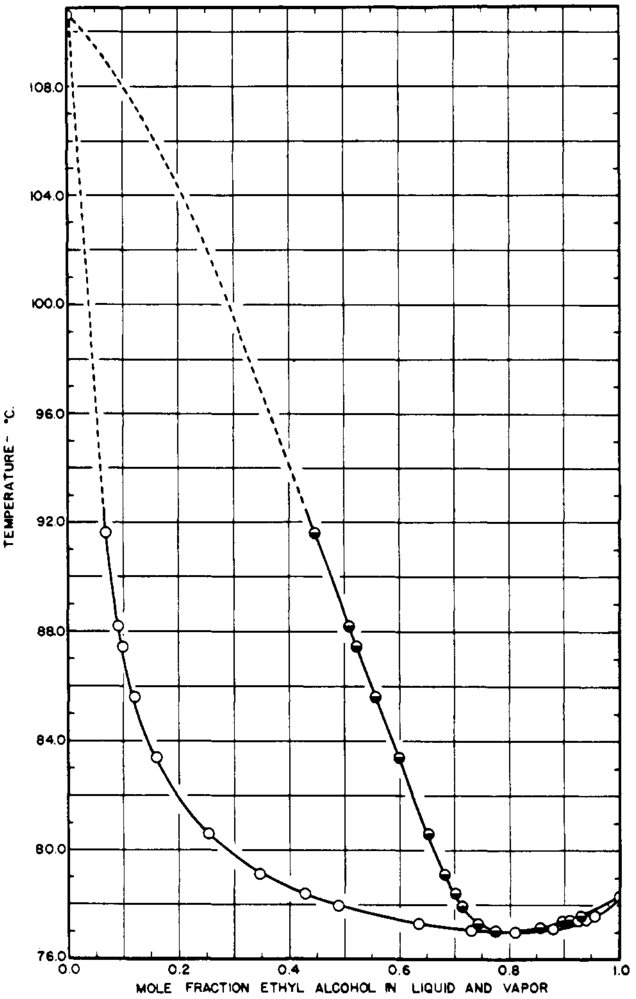

Figure 4. Temperature-composition diagram for toluene-ethyl alcohol system at 756 mm. of mercury

in Figures 6 and 7. Vapor pressure data were taken from (*5,7*).

The data were further analyzed by means of the Gibbs-Duhem equation. The equation

$$d\ln\gamma_1 = \frac{-x_2}{x_1}\, d\ln\gamma_2$$

was integrated graphically from $x_1 = 1.0$ to give

$$\ln\gamma_1 = \int \frac{-x_2}{x_1}\, d\ln\gamma_2$$

where subscript 1 refers to ethyl alcohol and subscript 2 refers to the hydrocarbon.

The results of these integrations are shown in Figures 6 and 7 as dotted lines.

DISCUSSION

The potentialities of the experimental method are well illustrated by Figure 8. Ten measurements of equilibrium data in the ethyl benzene-*n*-propyl alcohol system were made between a mole fraction in the liquid of 0.99 and 1.0. This part of the curve is very sensitive to experimental error and is for a system with high relative volatility. The precision of the results is seen to be mostly within ±0.1°C. and ±0.001 mole fraction unit.

The experimental *x-y* data for the ethyl alcohol-benzene system are compared with the published data on this system (*2, 6, 10*) in Figure 2. On the ethyl alcohol rich side of the diagram the authors' data fall somewhat above the mean of the published data. Otherwise, the comparison seems to be good. The ethyl alcohol-toluene system is compared with literature data (*11*) in Figure 3. The log activity coefficient curve for ethyl alcohol found by integrating the Gibbs-Duhem equation lies very close to the experimental curve except in the region below 15% of ethyl alcohol in the ethyl alcohol-toluene system. The deviation in this region is small. It is a consistent deviation not due to scatter in experimental data. This discrepancy between the experimental and integrated activity coefficient curves occurs only where a large temperature gradient exists in the system. This difference can be considerably reduced if a correction for nonisothermal conditions is applied to the Gibbs-Duhem equation.

This integration was performed using the heats of mixing

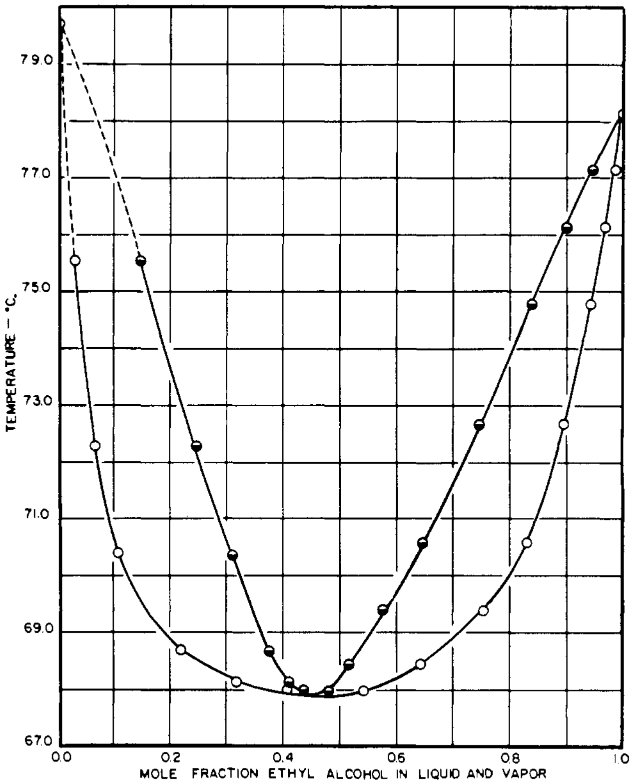

Figure 5. Temperature-composition diagram for benzene-ethyl alcohol system at 760 mm. of mercury

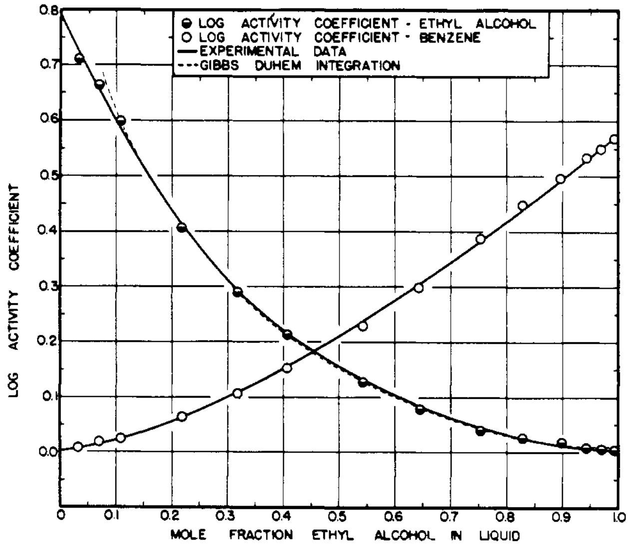

Figure 6. Diagram of log activity coefficient vs. composition for benzene-ethyl alcohol system at 760 mm. of mercury

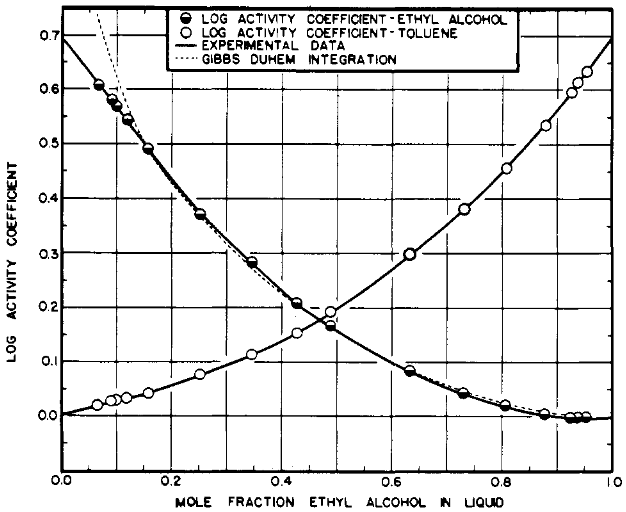

Figure 7. Diagram of log activity coefficient vs. composition for toluene-ethyl alcohol system at 765 mm. of mercury

data measured at 25° C. (9). The resulting curve lies approximately half-way between the experimental curve and the Gibbs-Duhem curve.

ACKNOWLEDGMENT

The authors wish to express their appreciation of the financial assistance of the Trustee's Research Fund of Rensselaer Polytechnic Institute. Robert Reynolds helped in the preparation of the diagrams.

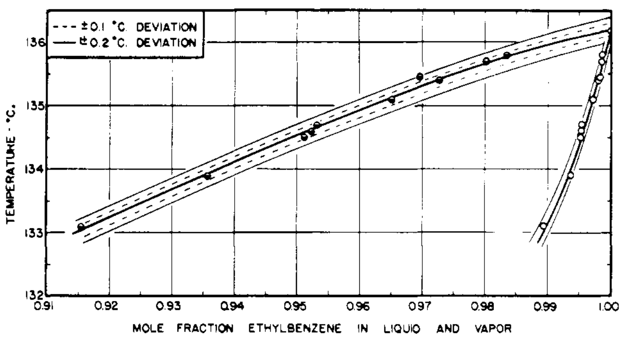

Figure 8. Temperature-composition diagram for ethylbenzene-n-propyl alcohol system

LITERATURE CITED

(1) Digney, F. J., Yerazunis, S., *Anal. Chem.* 25, 921 (1953).
(2) Ellis, S. R. M., *Trans. Inst. Chem. Engrs. (London)* 30, 58–64 (1952).
(3) Fowler, R. T., *J. Soc. Chem. Ind.* 68, 131 (1949).
(4) Gillespie, D. T. C., *Ind. Eng. Chem., Anal. Ed.* 18, 575 (1946).
(5) Lange, N. A., "Handbook of Chemistry," 4th ed., Handbook Publishers, Sandusky, Ohio, 1941.
(6) Perry, J. H., "Chemical Engineers' Handbook," 3rd ed., McGraw-Hill, New York, 1950.
(7) Stull, D. R., *Ind. Eng. Chem.* 39, 517 (1947).
(8) Timmermans, J., "Physico-Chemical Constants of Pure Organic Compounds," Elsevier, New York, 1950.
(9) Washburn, R. E., Lightbody, A., *J. Phys. Chem.* 34, 2701 (1930).
(10) Wehe, A. H., Coates, J., *Am. Inst. Chem. Engrs. Journal* 1, 241 (1955).
(11) Wright, W. A., *J. Phys. Chem.* 37, 233 (1933).

Received for review November 17, 1956. Accepted February 4, 1958.

Salt Effects in Aqueous Vapor-Liquid Equilibria

J. M. PRAUSNITZ and J. H. TARGOVNIK
Department of Chemical Engineering, University of California, Berkeley 4, Calif.

The addition of a salt to an aqueous solution of a volatile nonelectrolyte has a marked effect upon the vapor-liquid equilibria of the solution. The presence of the salt may either raise or lower the relative volatility of the nonelectrolyte or, in extreme cases, cause the formation of two liquid phases. The observed effects depend upon the nature and concentration of both the salt and nonelectrolyte.

Various experimental studies of the salt effect in vapor-liquid equilibria have been reported, but no concerted effort has been made to fit the results into a correlating framework.

THEORY

A charged particle superimposes many complications on the already complex water-nonelectrolyte interactions. The ions tend to attract and orient solvent molecules in a hydration shell around the ion, promote or destroy the short-range ordered structure of the water, and increase the internal pressure of the solution.

Theoretical explanations of the salt effect have been based upon various physical phenomena, notably electrostatic interactions, hydration, van der Waals forces, and internal pressure. These theoretical attempts, although not successful in describing the salt effect quantitatively except in severely restricted situations, are useful for interpreting data.

Electrostatic Effects. The first attempt to treat salting out as an electrostatic phenomenon was made by Debye and McAuley (*2*). Considering the ion as a perfect sphere of radius b, the Helmholtz work function, ΔA, is equal to the difference in the work of charging and discharging the ion in media of dielectric constants D and D_0, respectively, and the work done against the potential due to the ionic atmosphere. This leads to an equation which expresses the activity coefficient of the nonelectrolyte as a function of the ratio of charge to ionic radius, the ion concentration, and the decrement in the dielectric constant of the aqueous solution due to nonelectrolyte.

The equation of Debye and McAuley is based upon the assumptions that: the dielectric constant of the solution can be expressed as a linear function of salt concentration and nonelectrolyte concentration; salting out is due only to alterations in the dielectric constant of the solution; and the solution is dilute in both nonelectrolyte and salt. Estimation of the ionic radius in solution is very difficult, especially at moderate to high ion concentrations.

The electrostatic theory gives fairly good results for many dilute systems. However, it always predicts salting out and cannot account for salting in.

Internal Pressure. A contraction in volume usually follows the addition of a salt to water. By application of the principle of Tammann (*17*), an internal pressure, P_e, is defined. This principle proposes that a given amount of water in solution behaves like the same amount of pure water under a pressure greater than atmospheric. The work done in introducing a volume of nonelectrolyte V_i into a solution is then given by $P_e V_i$ and can be related to the Helmholtz-free-energy change.

It was shown (*13*) that as a result of these considerations the following expression can be obtained: